

Analyst

Accepted Manuscript



This is an *Accepted Manuscript*, which has been through the Royal Society of Chemistry peer review process and has been accepted for publication.

Accepted Manuscripts are published online shortly after acceptance, before technical editing, formatting and proof reading. Using this free service, authors can make their results available to the community, in citable form, before we publish the edited article. We will replace this *Accepted Manuscript* with the edited and formatted *Advance Article* as soon as it is available.

You can find more information about *Accepted Manuscripts* in the [Information for Authors](#).

Please note that technical editing may introduce minor changes to the text and/or graphics, which may alter content. The journal's standard [Terms & Conditions](#) and the [Ethical guidelines](#) still apply. In no event shall the Royal Society of Chemistry be held responsible for any errors or omissions in this *Accepted Manuscript* or any consequences arising from the use of any information it contains.

experiment. It can detect intracellular Al^{3+} in the contaminated living cell under a confocal fluorescence microscope. We also applied CN to the *in vivo* detection of Al^{3+} employing a living zebrafish.

Experiment

Equipments

^1H NMR and ^{13}C NMR spectra were recorded on Bruker Ultrashield 300 MHz NMR spectrometer. Chemical shifts were expressed in ppm (in DMSO-d_6 or CD_3OD ; TMS as internal standard) and coupling constants (J) in Hz. Mass spectroscopy was obtained from Micromass GC-TOF and Agilent Technologies 6540 UHD Accurate-Mass Q-TOF LC/MS. Fluorescence spectra were measured using Hitachi Fluorescence spectrophotometer-F-4600. The fluorescence lifetime was measured with a FLS 920 time-resolved spectroscope (Edinberge). Fluorescent images were captured by Olympus FV-1000 laser scanning confocal fluorescence microscope.

Chemicals

Methanol was HPLC grade. All of the other reagents were of analytical grade unless otherwise noted. $\text{Al}(\text{NO}_3)_3 \cdot 9\text{H}_2\text{O}$, LiClO_4 , NaCl , KCl , MgCl_2 , CaCl_2 , $\text{Fe}(\text{NO}_3)_2 \cdot 6\text{H}_2\text{O}$, $\text{FeCl}_3 \cdot 6\text{H}_2\text{O}$, $\text{CoCl}_2 \cdot 6\text{H}_2\text{O}$, $\text{Ni}(\text{NO}_3)_2 \cdot 6\text{H}_2\text{O}$, AgBF_4 , $\text{Cr}(\text{NO}_3)_3 \cdot 9\text{H}_2\text{O}$, $\text{Cd}(\text{NO}_3)_2 \cdot 4\text{H}_2\text{O}$, ZnCl_2 , $\text{Hg}(\text{ClO}_4)_2 \cdot 3\text{H}_2\text{O}$, $\text{CuCl}_2 \cdot 2\text{H}_2\text{O}$, $\text{Pb}(\text{NO}_3)_2$, $\text{Mn}(\text{NO}_3)_2$, GaCl_3 were employed in the selective experiment. For all aqueous solutions, deionized water purified by MilliQ Advantage Water Purification System was used.

Synthesis of 7-hydroxy-4-methyl-coumarin

4-Methylbenzenesulfonic acid (5 g) was added into the solution of resorcinol (11.0 g, 0.1 mol) in toluene (40 mL), and then acetoacetic ester (13.0 g) was added drop wise. The reaction mixture was refluxed for 3 h and monitored by TLC until the resorcinol was completely consumed. After cooling, the solution was poured into ice water (100 mL), yellow precipitate was collected by filtration and washed with cold water. Pale yellow solid was obtained by recrystallization with ethanol (11.3 g, Yield: 64 %). M.p. 185.0~186.0 °C. ^1H NMR (300 MHz, CD_3OD), d 7.61 (d, 1H, $J = 8.9$ Hz), 6.83 (d, 1H, $J = 10$ Hz), 6.70 (s, 1H), 6.10 (s, 1H), 2.42 (s, 3H). TOF MS EI calcd 176.0, found 176.0.

Synthesis of 7-hydroxy-4-methyl-6-nitro-2H-chromen-2-one

A solution of conc. Nitric acid (4.90 mL, 0.0775 mol) in concentrated sulphuric acid (5.1 mL) was added to a stirred solution of 7-hydroxy-4-methyl-coumarin (13.64 g, 0.0775 mol) in conc. sulphuric acid (30 mL) at such a rate as to keep the temperature below 5 °C. After warming to 20 °C, the reaction mixture was poured into a stirred mixture of ice cold water. The

yellow solid that separated was filtered and washed with hot ethanol thoroughly to get pure product. ^1H NMR (300 MHz, DMSO-d_6) δ 11.98 (s, 1H), 8.27 (s, 1H), 6.97 (s, 1H), 6.32 (d, $J = 0.8$ Hz, 1H), 2.40 (d, $J = 0.8$ Hz, 3H).

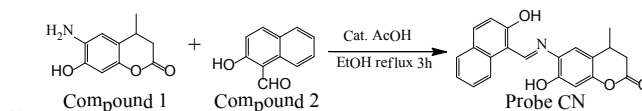
Synthesis of compound 1

Compound 1 was obtained from the hydrogenation carried out in a 100 mL stainless steel autoclave. 7-hydroxy-4-methyl-6-nitro-2H-chromen-2-one (663mg, 3 mmol), Pd-C (10%, 70mg) and EtOH (40ml) were added into the autoclave. The autoclave was flushed with hydrogen for three times to get rid of air. The hydrogenation reaction was performed under hydrogen atmosphere (6.0MPa) at 80°C and stirring at 300 r.p.m. for 5h. Then, the autoclave was cooled to the ambient temperature and flushed twice with nitrogen. Pd-C was filtered to get ethanol solution and conducted the next step without further treatment.

Synthesis of compound 2

Compound 2 was synthesized according to our previous procedures.

Synthesis of the probe CN



Scheme 1 Synthesis of probe CN

2-Hydroxy-naphthalene-1-carbaldehyde (516 mg, 3 mmol) and a drop of AcOH were added to the ethanol solution of 6-Amino-7-hydroxy-4-methyl-chroman-2-one obtained from the hydrogenation. Then the solution was refluxed for 3 h. After completion of the reaction, the obtained yellow precipitate was filtered and washed several times with cold ethanol to give CN (905 mg) as pure yellowish solid in 87% yield. ^1H NMR (300 MHz, DMSO-d_6) δ 15.88 (d, $J = 8.5$ Hz, 1H), 10.58 (s, 1H), 9.52 (d, $J = 8.5$ Hz, 1H), 8.40 (d, $J = 8.4$ Hz, 1H), 7.88 (s, 1H), 7.81 (d, $J = 9.4$ Hz, 1H), 7.69 (d, $J = 7.7$ Hz, 1H), 7.50 (t, $J = 7.4$ Hz, 1H), 7.28 (t, $J = 7.4$ Hz, 1H), 6.82 (d, $J = 9.3$ Hz, 1H), 6.66 (s, 1H), 3.19 (d, $J = 6.3$ Hz, 1H), 2.93 (dd, $J = 15.8, 5.5$ Hz, 1H), 2.60 (dd, $J = 15.9, 6.6$ Hz, 1H), 1.29 (d, $J = 6.9$ Hz, 3H). ^{13}C NMR (75 MHz, DMSO-d_6) δ 176.29, 168.46, 150.50, 149.52, 148.92, 137.90, 134.15, 129.46, 128.42, 126.45, 126.24, 124.92, 123.52, 120.30, 120.01, 116.31, 108.42, 104.36, 36.76, 28.96, 20.68. ESI-HRMS: calcd. for $(\text{C}_{21}\text{H}_{17}\text{NO}_4\text{-H})^-$ m/z 346.1079, found (M - H)⁻: 346.1087.

Cell culture

HeLa cells were cultured in Dulbecco's modified Eagle's medium (DMEM) containing 10% fetal bovine serum and antibiotics (100 units/mL penicillin and 100 $\mu\text{g}/\text{mL}$ streptomycin), maintaining at 37 °C in a humidified atmosphere of 95% air and 5% CO_2 .

Cell imaging

Fresh stock of HeLa cells was seeded into a glass bottom dish with a density of 1×10^5 cells per dish, and incubated for 24 h. Subsequently, the cells were exposed to 10 μM CN solution (900 μL DMEM mixed with 100 μL of 100 μM CN solution in EtOH) for 10 min at room temperature. The solution was then removed, and the cells were washed with PBS (2 mL \times 3) to clear CN molecules attached to the surface of cells. Afterwards, the cells were incubated for 15 min with 10 μM $\text{Al}(\text{NO}_3)_3$ DMEM solution at room temperature. The culture medium was removed, and the treated cells were washed three times with PBS (2 mL \times 3) before observation. Fluorescence imaging was performed with confocal laser scanning microscopy (Olympus, FV-1000; $\lambda_{\text{ex}}=458$ nm; fluorescent signals were collected at 480–580 nm). The images were captured using a photomultiplier.

Fluorescent detection of Al^{3+} in zebrafish

Zebrafish were kept at 28°C and maintained at optimal breeding conditions. For mating, male and female zebrafish were maintained in one tank at 28°C on a 12-h light/12-h dark cycle, and then the spawning of eggs was triggered by giving light stimulation in the morning. Almost all eggs were fertilized immediately. All stages of zebrafish were maintained in E3 embryo media (15 mM NaCl, 0.5 mM KCl, 1 mM MgSO_4 , 1 mM CaCl_2 , 0.15m M KH_2PO_4 , 0.05 mM Na_2HPO_4 , 0.7 mM NaHCO_3 , 5-10% methylene blue; pH 7.5). For imaging experiment, five-day-old zebrafish were incubated with 10 μM CN solution (900 μL DMEM mixed with 100 μL of 100 μM CN solution in EtOH) for 20 min at room temperature. The solution was then removed, and the cells were washed with PBS (2 mL \times 3) to clear CN molecules attached to the surface of zebrafish. Afterwards, the zebrafish were incubated for 20in with 40 μM $\text{Al}(\text{NO}_3)_3$ DMEM solution at room temperature. The culture medium was removed, and the treated cells were rinsed three times with PBS (2 mL \times 3) before observation. The treated zebrafish were imaged by confocal microscopy.

Results and discussion

Fluorescence response of the probe CN to different metal ions

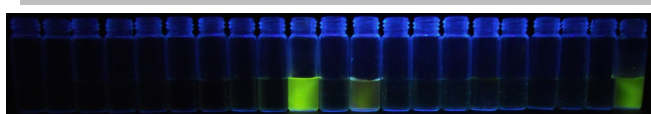


Fig.1 The fluorescent changes of CN (50 μM) in EtOH/Tris-HCl buffer (v/v, 1/9, pH=7.3) solutions upon addition of various metal ions (10 equiv) under excitation at 365 nm (hand-held UV lamp). Mix means CN with all kinds of metal ions.

When 10 equiv of various metal ions (Li^+ , Na^+ , K^+ , Mg^{2+} , Ca^{2+} , Fe^{2+} , Fe^{3+} , Co^{2+} , Ni^{2+} , Ag^+ , Cr^{3+} , Cd^{2+} , Zn^{2+} , Hg^{2+} , Cu^{2+} , Pb^{2+} , Mn^{2+} , Al^{3+} , Ga^{3+}) were added to 50 μM EtOH/Tris-HCl buffer (v/v, 1/9, pH=7.3) solutions of CN, it was found that Fe^{3+}

produced a color change from light yellow to light orange, which was probably caused by the chromogenic reaction of phenolic hydroxyl to Fe^{3+} . (Fig. S1). No change in color was observed upon the addition of other metal ions. The absorbance spectra of CN in presence and absence of Al^{3+} were shown in Fig. S3a. The molar extinction coefficient of CN was evaluated to be 1.98×10^4 $\text{L} \cdot \text{mol}^{-1} \cdot \text{cm}^{-1}$ (in the presence of Al^{3+}) and 1.80×10^4 $\text{L} \cdot \text{mol}^{-1} \cdot \text{cm}^{-1}$ (in the absence of Al^{3+}) respectively ($\lambda_{\text{max}}=442$ nm). Under excitation at 365 nm with a hand-held UV lamp, solution of the probe CN was nearly non-fluorescent (Fig.1). After the addition of Al^{3+} and Ga^{3+} , yellow-green and yellow fluorescence can be observed respectively. For the addition of Ga^{3+} , fluorescence intensity is relatively weaker in contrast with the addition of Al^{3+} . And the additions of other metal ions made no difference.

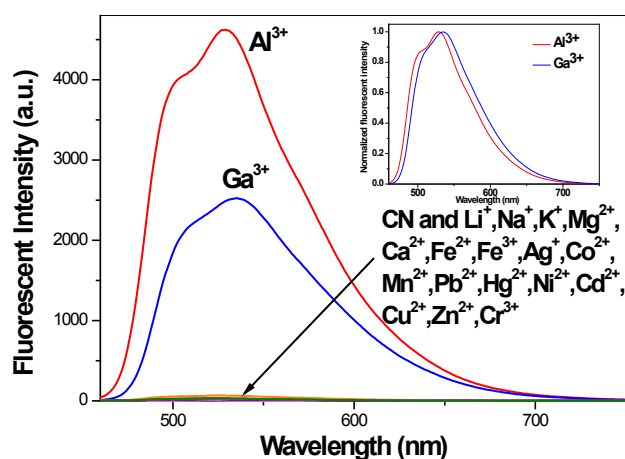


Fig.2 Fluorescence spectra of CN (10 μM) in EtOH/Tris-HCl buffer (v/v, 1/9, pH=7.3) with different metal ions upon excitation at 442 nm. Inset: Normalized fluorescence spectra of CN upon addition of Al^{3+} and Ga^{3+} .

To explore the utility of CN as ion-selectively fluorescent probe more accurately, fluorescence spectra of CN upon addition of various metal ions were measured. As shown in Fig.2, CN showed nearly no fluorescence upon excitation at 442 nm (excitation spectra in presence and absence of Al^{3+} were shown in Fig. S3b). Treatment with Al^{3+} induced a great increase in fluorescence intensity. Two emission peaks at 504 nm and 529 nm can be detected. Moreover, the addition of Ga^{3+} also resulted in an obvious enhancement of fluorescence with an emission peak at 535 nm. Thus, the 6 nm red-shift between Al^{3+} and Ga^{3+} caused fluorescent emissions, the different shapes of emission peaks and the various fluorescence intensities can be distinguishable enough for the probe to discriminate Al^{3+} and Ga^{3+} . The additions of other metal ions, Li^+ , Na^+ , K^+ , Mg^{2+} , Ca^{2+} , Fe^{2+} , Fe^{3+} , Co^{2+} , Ni^{2+} , Ag^+ , Cr^{3+} , Cd^{2+} , Zn^{2+} , Hg^{2+} , Cu^{2+} , Pb^{2+} , Mn^{2+} in our experiment, did nothing to the fluorescence of the probe. And particularly, Cr^{3+} , which always cannot be differentiated from Al^{3+} by many reported probes, still caused no change.

Fluorescence measurement

The quantitative fluorescence titration experiment was carried out using 10 μM CN in the presence of different concentrations of Al^{3+} from 0 to 5.0 equiv in EtOH/Tris-HCl buffer (v/v, 1/9, pH=7.3) solution. As shown in Fig. 3, CN exhibited remarkable fluorescence enhancements (~ 130 fold) at 504 nm and 529 nm respectively, with the quantum yields increasing from 0.003 to 0.51 (using quinoline as the reference with a known Φ value of 0.55 in 0.05 M H_2SO_4). This enhancement can be ascribed to the cation-induced inhibition of ESIPT process. The ESIPT process leads to very weak fluorescence.¹⁷ If the hydroxyls are coordinated with metal ions, metal coordination will remove this proton and inhibit the

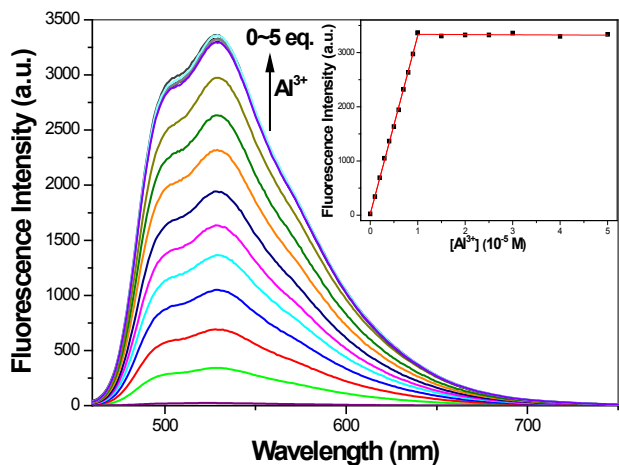


Fig.3 Fluorescence spectra of CN (10 μM) in EtOH/Tris-HCl buffer (v/v, 1/9, pH=7.3) solution in the presence of different concentrations of Al^{3+} (0, 0.1, 0.2, 0.3, 0.4, 0.5, 0.6, 0.7, 0.8, 0.9, 1.0, 1.5, 2.0, 2.5, 3.0, 4.0, 5.0 equiv) upon excitation at 442 nm. Inset: Fluorescence intensity changes at 529 nm.

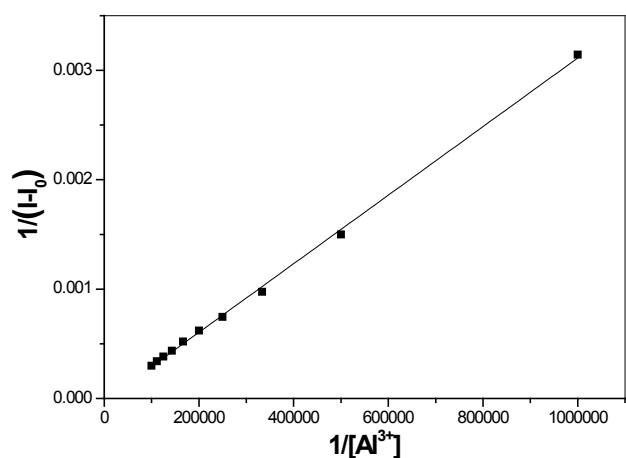


Fig.4 Benesi-Hildebrand plot of CN with Al^{3+} in EtOH/Tris-HCl buffer (v/v, 1/9, pH=7.3). The excitation wavelength was 442 nm and the observed wavelength was 529 nm.

ESIPT process, and a significant emission enhancement can be

observed.¹⁸ The luminescence lifetime of CN+ Al^{3+} was 2.75 ns in 529 nm (Fig. S4). After the concentrations of Al^{3+} increased up to 1.0 equiv, fluorescence intensities remained changeless. The association constant (K_a) was calculated to be $9.55 \times 10^4 \text{ M}^{-1}$ from a Benesi-Hildebrand plot¹⁹ (Fig.4, $R^2=0.99886$), demonstrating CN's strong binding capacity to Al^{3+} . To determine the detection limit of CN to Al^{3+} , fluorescence titration was conducted, employing 1 μM CN in the presence of different concentrations of Al^{3+} from 0 to 1.0 equiv in EtOH/Tris-HCl buffer (v/v, 1/9, pH=7.3) solution (Fig.5, $R^2=0.998$). The detection limit was evaluated to be as low as 0.10 μM .

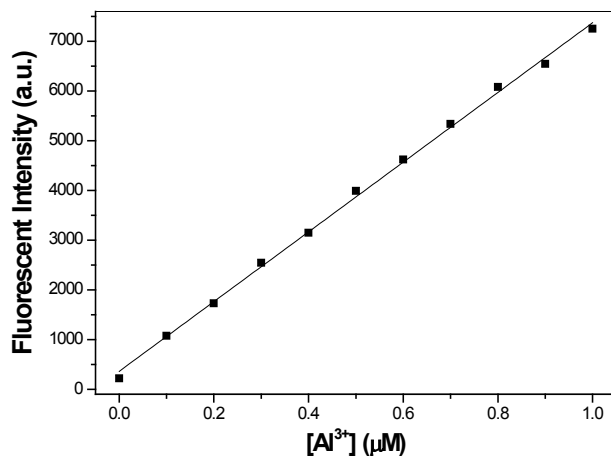


Fig.5 Fluorescence intensities at 529 nm of CN (1 μM) in EtOH/Tris-HCl buffer (v/v, 1/9, pH=7.3) solution as a function of $[\text{Al}^{3+}]$. The excitation wavelength was 442 nm and the observed wavelength was 529 nm.

Investigation of the binding mode

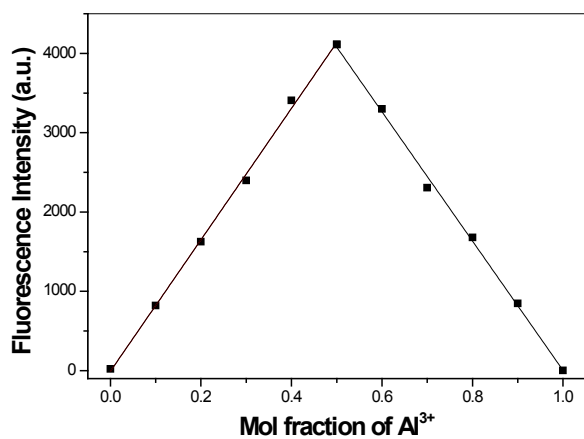
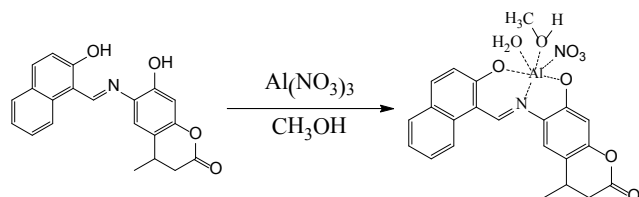


Fig.6 Job plot of the CN- Al^{3+} complexes in EtOH/Tris-HCl buffer (v/v, 1/9, pH=7.3) solution, keeping the total concentration of CN and Al^{3+} at 10 μM . The monitored wavelength was 516 nm.

In order to explore the binding stoichiometry between CN and Al^{3+} , Job plot experiment was conducted. As shown in Fig. 6, the fluorescence intensities at 529 nm were plotted against the molar

fractions of Al^{3+} keeping the total contraction constant ($10\mu\text{M}$). The maximum fluorescence intensity, when the molar fraction of Al^{3+} was 0.5, indicated a 1:1 stoichiometry for CN- Al^{3+} complexes. In addition, the ESI-MS (negative mode) data (Fig. S2) of the complex showed $m/z=967.00$ for CN with Al^{3+} , corresponding to $[\text{2}(\text{CN}-2\text{H}^+ + \text{Al}^{3+} + \text{MeOH} + \text{NO}_3^- + \text{H}_2\text{O}) - \text{H}^+]^-$ (calc. for 967.20), and confirmed a 1:1 stoichiometry for the CN- Al^{3+} complex. The proposed structure of CN- Al^{3+} complex was shown in Scheme 2.



Scheme 2 Proposed structure of CN- Al^{3+} complex.

Competition experiment and the effect of pH

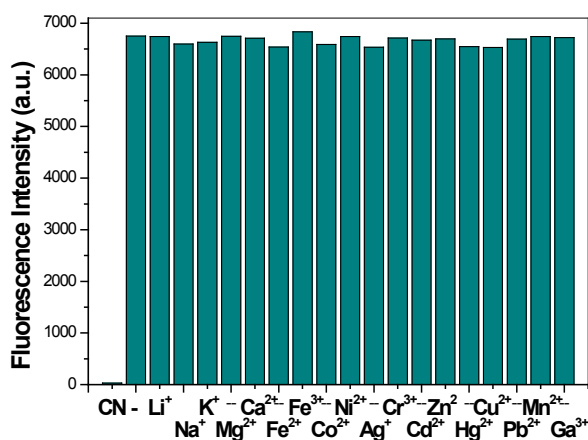


Fig. 7 Competition experiment of CN towards Al^{3+} (1 equiv) in the absence or presence of various metal ions (K^+ , Na^+ , Ca^{2+} were 50 equiv, others were 10 equiv). Excitation wavelength was 442 nm, emission wavelength was 529 nm.

To examine the selectivity for Al^{3+} in a complex background of potentially competing species, the fluorescence enhancement of CN with Al^{3+} was investigated in the presence of other metal ions. When CN was treated with 1 equiv of Al^{3+} in the presence of various metal ions (K^+ , Na^+ , Ca^{2+} were 50 equiv, others were 10 equiv), the fluorescent enhancements caused by Al^{3+} was retained with all the other kinds of metal ions (Fig. 7). Particularly, Fe^{3+} and Cu^{2+} also did not quench the fluorescence of CN enhanced by Al^{3+} , which was a common phenomenon in many reported Al^{3+} turn-on probe. Furthermore, the cross-sensitivity to K^+ , Na^+ , Ca^{2+} (50 equiv) indicated that the probe would perform well in living cells in which the activities of K^+ , Na^+ and Ca^{2+} could be quite high.

Moreover, to test the application extent of CN as Al^{3+} probe,

fluorescent properties of CN in the absence and presence of Al^{3+} were investigated at different pH values. As shown in Fig. 8, CN showed nearly no fluorescence in the pH range of 2-12. In the presence of 1 equiv Al^{3+} , the fluorescence would not be influenced by the acidic or neutral environment with a pH range of 2-7. However, as the alkalinity increased, the fluorescence intensity decreased greatly because the formation of $\text{Al}(\text{OH})_3$ reduced the concentration of Al^{3+} in solution. When the pH value increased to 8.6, no enhanced signal could be detected. To exclude the possibility of the decreased fluorescence caused by the decomposition of the probe, we examined the stability of CN under basic environment. The probe was kept in the solution (pH=7.2 and 12) for 24 h, and no new compound could be detected through thin-layer chromatography (TLC), indicating that CN was stable under basic environment. Thus, the decreased fluorescence should be ascribed to the transformation of $\text{Al}(\text{OH})_3$.

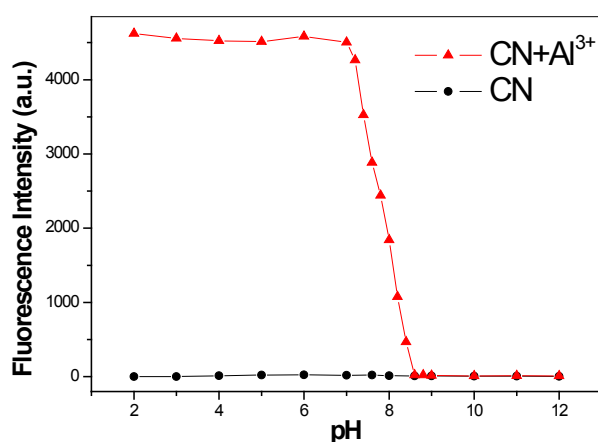


Fig. 8 Fluorescence intensity of ZS1 ($10\mu\text{M}$) at various pH values in EtOH/Tris-HCl buffer (v/v, 1/9, pH=7.3) solution, in the absence and presence of Al^{3+} (1 equiv). Excitation wavelength was 442 nm, emission wavelength was 529 nm.

Imaging of intracellular Al^{3+}

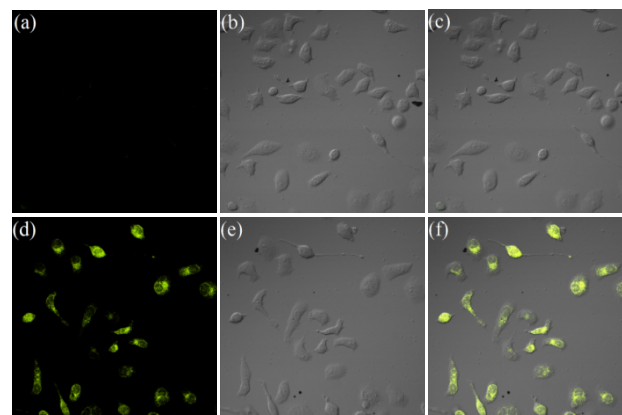


Fig. 9 Fluorescence images of Al^{3+} in HeLa cells using probe CN upon excitation at 458 nm. (a) Fluorescent image, (b) bright field image and (c) bright field image of cells without probe; (d) Fluorescent image, (e) bright field image and (f) bright field image of cells with probe.

merged image of HeLa cells incubated with probe CN (10 μM) for 20 min. (d) Fluorescent image, (e) bright field image and (f) merged image of HeLa cells incubated with Al^{3+} (20 μM) for 20 min after treating with probe CN.

Then, the potential of bioimaging application of CN for sensing Al^{3+} in living cells was investigated. The images of cells were obtained using a confocal fluorescence microscope. When HeLa cells were incubated with CN (10 μM) for 20 min at room temperature, nearly no fluorescence could be observed (Fig.9a). After the treated cells were incubated with Al^{3+} (20 μM) in the culture medium for 20 min at room temperature, bright yellow-green fluorescence was observed in the HeLa cells (Fig.9d). Moreover, the merged picture (Fig.9f) confirms that the fluorescence signals are only located in the intracellular area. Moreover, cell morphology remained in fine condition after intake of CN, indicating the great cytocompatibility and low toxicity of the probe. Accordingly, the probe CN is cell membrane permeable and could be applied for detecting Al^{3+} within living cells.

Imaging Al^{3+} in zebrafish

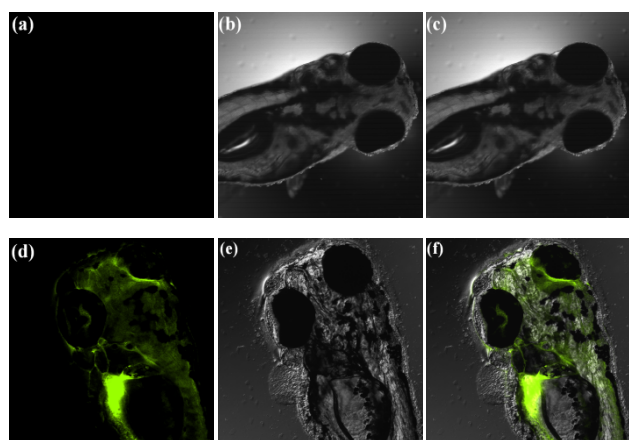


Fig.10 Fluorescence images of Al^{3+} in zebrafish using probe CN upon excitation at 458 nm. (a)Fluorescent image, (b) bright field image and (c) merged image of zebrafish incubated with probe CN (10 μM) for 20 min. (d) Fluorescent image, (e) bright field image and (f) merged image of CN-loaded zebrafish incubated with Al^{3+} (20 μM) for 20 min.

A further exploratory effort was made to determine if probe CN could be used for imaging Al^{3+} in zebrafish. As shown in Fig. 12, five-day-old zebrafish, treated with probe CN (10 μM) for 20 min at room temperature, showed very weak fluorescence (Fig. 10a). Moreover, the CN-loaded zebrafish treated with 40 μM Al^{3+} give a strong yellow-green fluorescence (Fig. 10d). These *in vivo* studies indicated that probe CN is suited for monitoring the distribution of Al^{3+} in living bodies.

Conclusions

In summary, an easily synthesized coumarin-based Al^{3+} selective fluorescent probe CN was synthesized and characterized. The binding mode was proved to be 1:1 and the detection limit was

calculated to be as low as 0.10 μM . CN could be applied to detecting Al^{3+} in living cells, and studies towards the *in vivo* detection of Al^{3+} were also carried out successfully using a living zebrafish.

Acknowledgments

This work was supported by the National Basic Research Program of China (No.2014CD846004) and Jiangsu Province Science Technology Innovation and Achievements Transformation Special Fund (BY2012149).

Notes and references

- (a) R. Azadbakht and J. Khanabadi, *Inorg. Chem. Comm.*, 2013, **30**, 21–25; (b) Y. M. Yang, Q. Zhao, W. Feng, F. Y. Li, *Chem. Rev.*, 2013, **113**, 192–270.
- (a) X. B. Huang, Y. Dong, Q. W. Huang, Y. X. Cheng, *Tetrahedron Letters*, 2013, **54**, 3822–3825; (b) Q. Y. Cao, Y. M. Han, H. M. Wang, Y. Xie, *Dyes and Pigments*, 2013, **99**, 798–802; (c) C. J. Gao, X. J. Jin, X. H. Yan, P. An, Y. Zhang, L. L. Liu, H. Tian, W. S. Liu, X. J. Yao, Y. Tang, *Sensors and Actuators B*, 2013, **176**, 775–781.
- S. Banthia and A. Samanta, *J. Phys. Chem. B*, 2006, **110**, 6437–6440.
- (a) N. Singh, N. Kaur, R. C. Mulrooney and J. F. Callan, *Tetrahedron Letters*, 2008, **49**, 6690–6692; (b) K. Tiwari, M. Mishra and V. P. Singh, *RSC Adv.*, 2013, **3**, 12124–12132; (d) S. Goswami, S. Paul and A. Manna, *RSC Adv.*, 2013, **3**, 10639–10643.
- W. H. Ding, W. Cao, X. J. Zheng, D. C. Fang, W. T. Wong and L. P. Jin *Inorg. Chem.*, 2013, **52**, 7320–7322.
- (a) K. Ando, S. Hayashi, S. Kato, *Phys. Chem. Chem. Phys.*, 2011, **13**, 11118; (b) C. C. Hsieh, C. M. Jiang, P. T. Chou, *Acc. Chem. Res.*, 2010, **43**, 1364; (c) G. Y. Li, G. J. Zhao, Y. H. Liu, K. L. Han, G. Z. He, *J. Comput. Chem.*, 2010, **31**, 1759; (d) J. N. Li, M. Pu, D. C. Fang, M. Wei, J. He, D. E. Evans, *J. Mol. Struct.*, 2012, **1015**, 106; (e) G. Gui, Z. Lan, W. Thiel, *J. Am. Chem. Soc.*, 2012, **134**, 1662.
- E. Oliveira, H. M. Santos, J. L. Capelo, C. Lodeiro, *Inorg. Chim. Acta*, 2012, **381**, 203–211.
- G. Frantzios, B. Galatis and P. Apostolakos, *New Phytol.*, 2000, **145**, 211–214.
- B. Valeur and I. Leray, *Coord. Chem. Rev.*, 2000, **205**, 3–40.
- (a) G. D. Fasman, *Coord. Chem. Rev.*, 1996, **149**, 125; (b) P. Nayak, *Environ. Res.*, 2002, **89**, 101.
- (a) C. S. Cronan, W. J. Walker and P. R. Bloom, *Nature*, 1986, **324**, 140; (b) G. Berthon, *Coord. Chem. Rev.*, 2002, **228**, 319.
- C. Stephen, W. Smith, S. Heng, H. E. Heidepriem, D. A. Abell and T. M. Monro, *Langmuir*, 2011, **27**, 5680–5685.
- N. E. W. Alstad, B. M. Kjelsberg, L. A. Vollestad, E. Lydersen and A. B. S. Poléo, *Environ. Pollut.*, 2005, **133**, 333.
- (a) Y. Zhao, Z. Lin, H. Liao, C. Duan, Q. Meng, *Inorg. Chem. Commun.*, 2006, **9**, 966–968. (b) K. Soroka, R. S. Vithanage, D. A. Phillips, B. Waker, P. K. Dasgupta, *Anal. Chem.*, 1987, **59**, 629–636.
- (a) X. Sun, Y. W. Wang and Y. Peng, *Org. Lett.*, 2012, **14**, 3420–3423; (b) A. Sahana, A. Banerjee, S. Lohar, B. Sarkar, S. K. Mukhopadhyay and D. Das, *Inorg. Chem.*, 2013, **52**, 3627–3633; (c) S. Kim, J. Y. Noh, K. Y. Kim, J. H. Kim, H. K. Kang, S. W. Nam, S. H. Kim, S. Park, C. Kim and J. H. Kim, *Inorg. Chem.*, 2012, **51**, 3597–3602; (e) S. Guha, S. Lohar, A. Sahana, Ar. B. erjee, D. A. Safin, M. G. Babashkina, M. P. Mitoraj, M. Bolte, Y. Garcia, S. K. M. adhyay and D. Das, *Dalton Trans.*, 2013, **42**, 10198–10207; (f) Y. K. Jang, U. C. Nam, H. L. Kwon, I. H. Hwang, C. Kim, *Dyes and Pigments*, 2013, **99**, 6–13; (g) S. B. Maity and P. K. Bharadwaj, *Inorg. Chem.*, 2013, **52**, 1161–1163; (h) J. Y. Jung, S. J. Han, J. H. Chun, C. M. Lee, J. Y. Yoon, *Dyes and Pigments*, 2012, **94**, 423–426; (i) L. Y. Wang, H. H. Li, D. R. Cao, *Sensors and Actuators B*, 2013, **181**, 749–755; (j) S. B. Maity and P. K. Bharadwaj, *Inorg. Chem.*, 2013, **52**, 1161–1163; (k) J. Y. Jung, S. J. Han, J. H. Chun, C. M.

-
- Lee, J. Y Yoon, *Dyes and Pigments*, 2012, **94**, 423–426; (l) L. Y. Wang, H. H. Li, D. R. Cao, *Sensors and Actuators B*, 2013, **181**, 749–755; (m) B. Jisha, M. R. Resmi, R. J. Maya, R. Luxmi Varma, *Tetrahedron Letters*, 2013, **54**, 4232–4236.
- 16 L. Jiang, L. Wang, M. Guo, G. Yin, R. Y. Wang, *Sensors and Actuators B*, 2011, **156**, 825–831.
- 17 (a) J. S. Wu, W. M. Liu, J. C. Ge, H. Y. Zhang and P. F. Wang, *Chem. Soc. Rev.*, 2011, **40**, 3483–3495; (b) M. M. Henary, C. Fahrni, *J. J. Phys. Chem. A*, 2002, **106**, 5210–5220.
- 18 M. M. Henary, Y. G. Wu and C. J. Fahrni, *Chem. Eur. J.*, 2004, **10**, 3015–3025.
- 19 H. A. Benesi and J. H. Hildebrand, *J. Am. Chem. Soc.*, 1949, **71**, 2703–2707.